The Abdus Salam
International Centre for Theoretical Physics

United Nations
Educational, Scientific and
Cultural Organization

IAEA
International Atomic Energy Agency

1984-4

International Workshop on Advanced Polymer Science and Turbulent Drag Reduction

10 - 20 March 2008

Turbulent Drag Reduction by Dilute Addition of High Polymers: Theory, Experiments, Simulations and Predictions

Jovan JOVANOVIC
LSTM
Friedrich-Alexander University
Cauerstrasse 4
D-91058 Erlangen-Nuremberg
GERMANY

Turbulent Drag Reduction by Dilute Addition of High Polymers: Theory, Experiments, Simulations and Predictions

Jovan Jovanović
LSTM, Chair of Fluid Mechanics
Friedrich-Alexander University
Erlangen-Nuremberg, Germany

Bettina Frohnapfel
Turbulence and Heat Transfer
Laboratory Department of
Mechanical Engineering
The University of Tokyo

Peter Lammers
High Performance
Computing Center Stuttgart
NobelStr.19, 70569 Stuttgart

Scope of the Presentation

- Turbulent drag reduction by dilute addition of high polymers
- Review of turbulence research
- Invariant modeling of turbulence
- The limiting state of turbulence at the wall
- Polymer-turbulence interaction
- Parameterization of polymer-turbulence interaction for maximum drag reduction effect
- Further examples of turbulent drag reduction and related flow phenomena
- Turbulent drag reductions by surface-embedded grooves
- Conclusions and final remarks

Flow control

Drag Reduction (DR)

minimize drag force
- separation control (control pressure drag)
- skin friction control

Long chain polymers in turbulent wall bounded flows

- turbulent DR up to 80% with a few ppm of polymer
- act in turbulent boundary layer

Application Area:

Transalaska Pipeline: 30% energy savings

The energy dissipation rate

The average energy dissipation rate $\overline{\Phi}$ can be expressed as the work done against the wall shear stress τ_w per unit mass of fluid:

$$\overline{\Phi} \qquad \overline{\Phi}$$

$$\frac{1}{V}\int \rho \left[\nu \left(\frac{d\overline{U_1}}{dx_2} \right)^2 + \nu \overline{\frac{\partial u_i}{\partial x_k}\frac{\partial u_i}{\partial x_k}} \right] dV \cong \frac{A_w \tau_w U_B}{\rho V}$$

$$\varepsilon \sim \nu_t \left(\frac{d\overline{U_1}}{dx_2} \right)^2$$

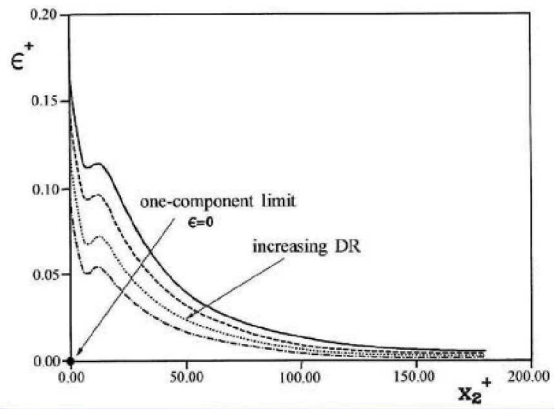

$$\varepsilon \cong \frac{u_\tau^3}{\kappa x_2}$$

Distribution of the turbulent dissipation rate versus difference from the wall

Some historical comments on turbulence

• **O. Reynolds**	**(1895)**
• ***L. Prandtl***	***(1925)***
• G. Taylor	(1935)
• Th. Von Karman	(1930)
• H. L. Dryden • G. B. Shubauer • H. K. Skramstad	(1940)
• **A. N. Kolmogorov**	**(1941)**
• **P. Y. Chou**	**(1945)**
• G. K. Batchelor	(1946-1962)
• A. A. Townsend	(1947-)
• ***J. Rotta***	***(1951)***
• E. Hopf	(1952)
• R. E. Kraichnan	(1953)
• J. Laufer	(1954)
• P. S. Klebanoff	(1955)
• ***B. I. Davidov***	***(1961)***
• S. Corrsin	(1942 - 1985)
• L. G. Kovasznay	(1959 - 1980)
• P. Bradshaw	(1965 -)
• F. H. Harlow	(1965)
• ***B. Spalding***	***(1965 - 1975)***
• S. Kline • W. C. Reynolds • W. Rundstadler	(1967)
• **J. L. Lumley**	**(1967 -)**
• J. W. Deordorff	(1970)
• S. A. Orszag	(1972)
• U. Schumann	(1973)
• ***R. S. Rogallo***	***(1981)***

The turbulence closure problem

Turbulence decomposition suggested by O. Reynolds (1895):

$$U_i = \overline{U}_i + u_i \quad , \quad P = \overline{P} + p$$

when applied to the Navier-Stokes equations leads to the closure problem

- $$\frac{\partial \overline{U}_i}{\partial t} + \overline{U}_k \frac{\partial \overline{U}_i}{\partial x_k} = -\frac{1}{\rho}\frac{\partial \overline{P}}{\partial x_i} + \frac{\partial}{\partial x_k}\left(\nu \frac{\partial \overline{U}_i}{\partial x_k} - \underbrace{\overline{u_i u_k}}_{?}\right), \qquad \frac{\partial \overline{U}_i}{\partial x_i} = 0$$

- $$\frac{\partial \overline{u_i u_j}}{\partial t} + \overline{U}_k \frac{\partial \overline{u_i u_j}}{\partial x_k} = -\overline{u_j u_k}\frac{\partial \overline{U}_i}{\partial x_k} - \overline{u_i u_k}\frac{\partial \overline{U}_j}{\partial x_k} - \overbrace{\frac{\partial \overline{u_i u_j u_k}}{\partial x_k}}^{T_{ij}?} - \overbrace{\frac{1}{\rho}\left(\overline{u_j \frac{\partial P}{\partial x_i}} + \overline{u_i \frac{\partial P}{\partial x_j}}\right)}^{\Pi_{ij}?} - \overbrace{2\nu \overline{\frac{\partial u_i}{\partial x_k}\frac{\partial u_j}{\partial x_k}}}^{\epsilon_{ij}?} + \nu \frac{\partial^2 \overline{u_i u_j}}{\partial x_k \partial x_k}$$

- $$\frac{\partial \overline{u_i u_j u_\ell}}{\partial t} + \overline{U}_k \frac{\partial \overline{u_i u_j u_\ell}}{\partial x_k} = \overline{u_i u_j}\frac{\partial \overline{u_\ell u_k}}{\partial x_k} + \overline{u_j u_\ell}\frac{\partial \overline{u_i u_k}}{\partial x_k} + \overline{u_\ell u_i}\frac{\partial \overline{u_j u_k}}{\partial x_k} - \overline{u_j u_\ell u_k}\frac{\partial \overline{U}_i}{\partial x_k} - \overline{u_i u_j u_k}\frac{\partial \overline{U}_\ell}{\partial x_k} - \overline{u_\ell u_i u_k}\frac{\partial \overline{U}_j}{\partial x_k}$$
$$- \underbrace{\frac{\partial \overline{u_i u_j u_\ell u_k}}{\partial x_k}}_{T_{ijl}?} - \underbrace{\frac{1}{\rho}\left(\overline{u_\ell u_j \frac{\partial P}{\partial x_i}} + \overline{u_\ell u_j \frac{\partial P}{\partial x_j}} + \overline{u_i u_j \frac{\partial P}{\partial x_\ell}}\right)}_{\Pi_{ijl}?} - \underbrace{2\nu\left(\overline{u_i \frac{\partial u_j}{\partial x_k}\frac{\partial u_\ell}{\partial x_k}} + \overline{u_j \frac{\partial u_i}{\partial x_k}\frac{\partial u_\ell}{\partial x_k}} + \overline{u_\ell \frac{\partial u_i}{\partial x_k}\frac{\partial u_j}{\partial x_k}}\right)}_{\epsilon_{ijl}?} + \nu \frac{\partial^2 \overline{u_i u_j u_\ell}}{\partial x_k \partial x_k}$$

- .....

Kolmogorov's model of turbulence (1942)

Kolmogorov's two-equation model of turbulence

$$\frac{D\overline{v_i}}{Dt} = F_i - \frac{\partial}{\partial x_i}\left(\frac{\overline{p}}{\varrho} + b\right) + A\sum_j \frac{\partial}{\partial x_j}\left[\frac{b}{\omega}\left(\frac{\partial \overline{v}_i}{\partial x_j} + \frac{\partial \overline{v}_j}{\partial x_i}\right)\right]$$

$$\boxed{\frac{D\omega}{Dt} = -\frac{7}{11}\omega^2 + A'\sum_j \frac{\partial}{\partial x_j}\left[\frac{b}{\omega}\frac{\partial \omega}{\partial x_j}\right]}$$

$$\frac{Db}{Dt} = -b\omega + \frac{A}{3}\frac{b}{\omega}\epsilon + A''\sum_j \frac{\partial}{\partial x_j}\left[\frac{b}{\omega}\frac{\partial \epsilon}{\partial x_j}\right]$$

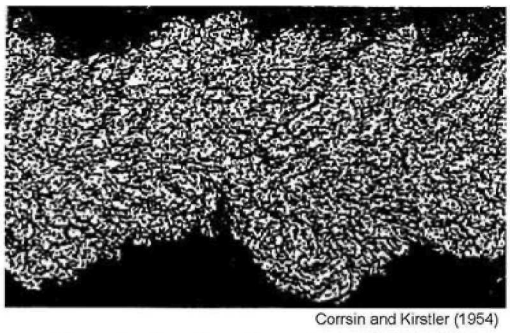

Corrsin and Kirstler (1954)

Flow visualisation of small-scale structure of turbulence at large *Re*

The missing source term in the ω equation:

One of the central unresolved issues in the formulation of the closure approximations involved in the dynamic equations for the turbulent dissipation rate is related to the early work on turbulence theory reported by Kolmogorov (1942). In his pioneering paper, which nowadays stands as a pattern for the two-equation model of turbulence, he omitted the production terms in the equation for the characteristic frequency ω of the energy-containing range, which served for determination of the turbulent dissipation rate.

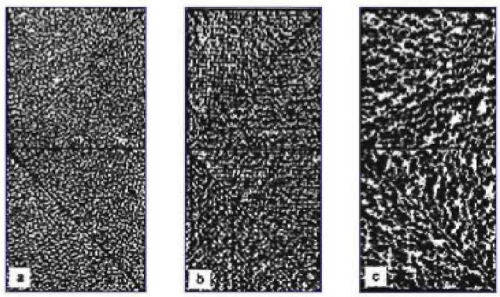

Tennekes and Lumley (1972)

(a) Isotropic pattern, (b) and (c) are anisotropic patterns

Turbulence closure proposed by Chou (1945)

Quarterly of Applied Mathematics
Vol. III, No. 1, **1945**

ON VELOCITY CORRELATIONS AND TUE SOLUTIONS OF THE EQUATIONS OF TURBULENT FLUCTUATLON*

BY

P. Y. CHOU**

National Tsing Iiua University, Kunming, China

$$\frac{\partial \overline{U}_i}{\partial t} + \overline{U}^j \overline{U}_{i,j} = -\frac{1}{\varrho}\bar{p}_{,i} + \frac{1}{\varrho}\tau^j_{i,j} + \nu\nabla^2 \overline{U}_i\,, \qquad \overline{U}^j{}_{,j} = 0$$

$$-\frac{1}{\varrho}\frac{\partial \tau_{ik}}{\partial t} - \frac{1}{\varrho}(\overline{U}_{i,j}\tau^j_k + \overline{U}_{k,j}\tau^j_i) - \frac{1}{\varrho}\overline{U}^j\tau_{ik,j} + (\overline{w^j w_i w_k})_{,j} = -a^n_{mik}\overline{U}^m_{,n} - b_{ik} - \frac{\nu}{\varrho}\nabla^2\tau_{ik} + \frac{2\nu}{3\lambda^2}(k-5)q^2 g_{ik} - \frac{2\nu k}{\lambda^2}\overline{w_i w_k},$$

$$5\frac{\partial}{\partial t}\left(\frac{q^2}{\lambda^2}\right) + 5\overline{U}^j\frac{\partial}{\partial x^j}\left(\frac{q^2}{\lambda^2}\right) - \frac{14G}{\lambda^2}\overline{U}_{i,k}\overline{w^i w^k} - \frac{70F}{3\sqrt{3}}\frac{q^3}{\lambda^3} = -\frac{2\nu}{3}E\frac{q^2}{\lambda^4},$$

$$\frac{\partial}{\partial t}\overline{w_i w_k w_l} + \overline{U}_{i,j}\overline{w^j w_k w_l} + \overline{U}_{k,j}\overline{w^j w_l w_i} + \overline{U}_{l,j}\overline{w^j w_i w_k} + \overline{U}^j(\overline{w_i w_k w_l})_{,j} + (\overline{w^j w_i w_k w_l})_{,j} =$$

$$-b^n_{mikl}\overline{U}^m_{,n} - c_{ikl} + \frac{1}{\varrho^2}(\tau^j_{i,j}\tau_{kl} + \tau^j_{k,j}\tau_{li} + \tau^j_{l,j}\tau_{ki}) + \nu g^{mn}(\overline{w_i w_k w_l})_{,mn},$$

Invariant modelling of turbulence

J. L. Lumley and G. R. Newman

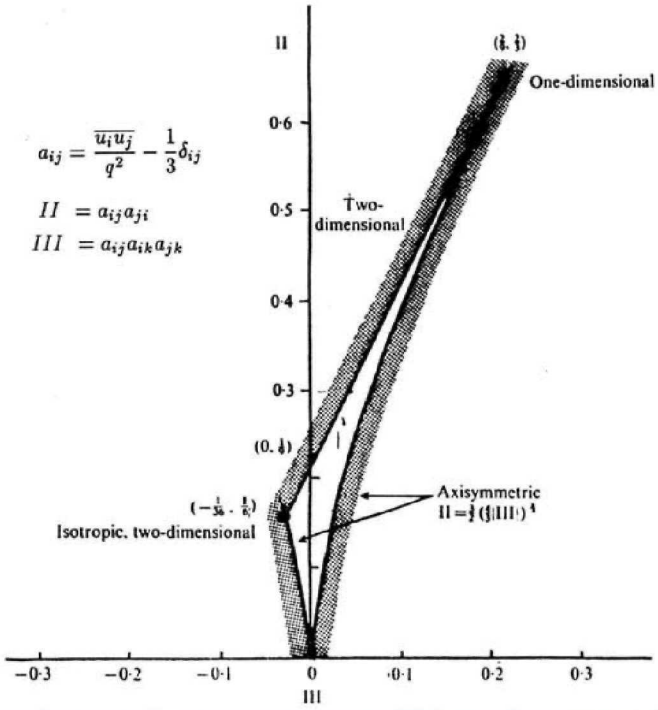

$$a_{ij} = \frac{\overline{u_i u_j}}{q^2} - \frac{1}{3}\delta_{ij}$$

$$II = a_{ij}a_{ji}$$

$$III = a_{ij}a_{ik}a_{jk}$$

Invariant theory of Lumley (1977)

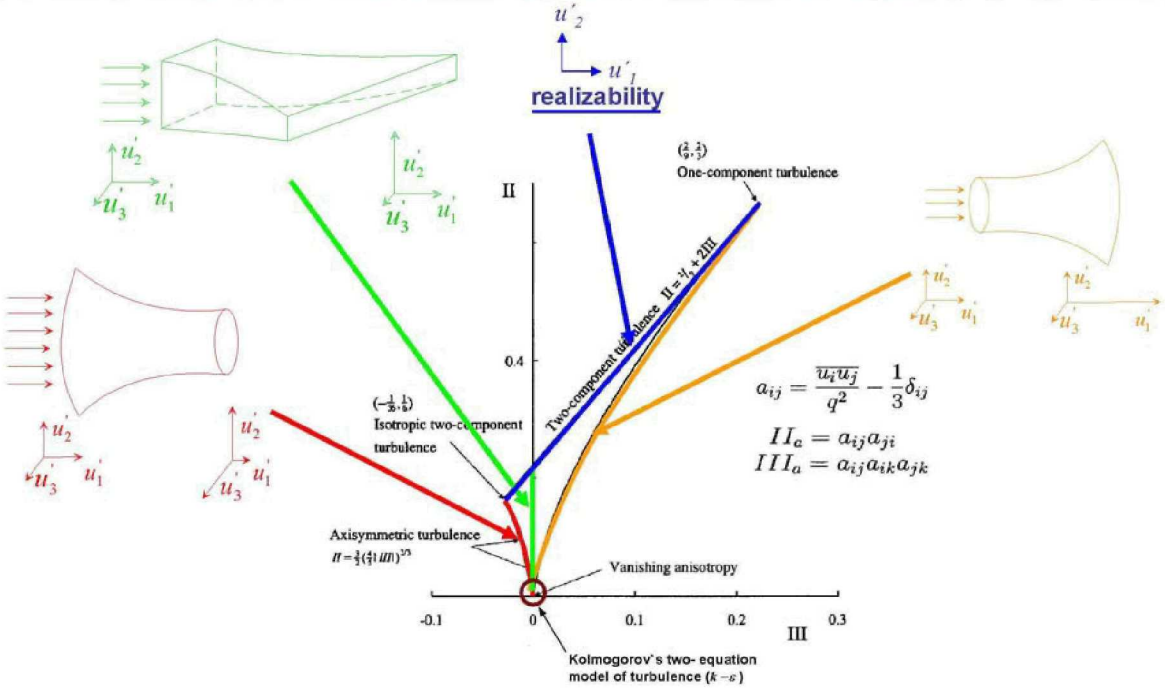

$$a_{ij} = \frac{\overline{u_i u_j}}{q^2} - \frac{1}{3}\delta_{ij}$$

$$II_a = a_{ij}a_{ji}$$

$$III_a = a_{ij}a_{ik}a_{jk}$$

All realizable turbulence must be inside the triangle: Lumley (1978)

Numerical databases used to validate the turbulence closure

Reference	Flow	Reynolds number
Rogallo (1981) Lee (1985)	Homogeneous turbulence	
	Plain strain (B2D1,B2D2,B2D3 and B2D4)	$R_\lambda \simeq 28$-40
	Axisymmetric contraction (CD11,CD12,CD13, CD14,CD21,CD22, CD23 and CD24)	$R_\lambda \simeq 10$-20
	Shear (BSH9,BSH10, BSH11and BSH12)	$R_\lambda \simeq 40$-120
	Rotation (BR1,BR2,BR3, BR4 and BR6)	$R_\lambda \simeq 13$-18
	Relaxation to isotropy (RX11A,...,RX24A, RX11C,...,RX24C, RX11F,...,RX24F)	$R_\lambda \simeq 7$-22

Reference	Flow	Reynolds number
Kim, Moin & Moser (1987)	Channel flow	$R_e \simeq 3250$
Antonia *et al.* (1992)	Channel flow	$R_e \simeq 7880$
Gilbert & Kleiser (1991)	Channel flow	$R_e \simeq 3830$
Kasagi *et al.* (1990)	Channel flow	$R_e \simeq 1740, 2680, 3240$
Moser, Kim & Mansour (1998)	Channel flow	$R_e \simeq 12500$
Eggels *et al.* (1994)	Pipe flow	$R_e \simeq 6950$
Eggels, Boersma & Nieuwstadt (1994)	Rotating pipe flow	$R_e \simeq 5300, 5575, 5860$ $N = 0., 0.32, 0.61$
Orlandi & Fatica (1997)	Rotating pipe flow	$R_e \simeq 5000$ $N = 0., 0.5, 1.0, 2.0$
Spalart (1988)	Boundary layer	$R_\theta \simeq 300, 670, 1410$
Spalart (1986)	Sink flow	$R_\theta \simeq 380, 415, 690$
Le & Moin (1994)	Backward-facing step	$R_e \simeq 5100$
Rogers & Moser (1994)	Plane mixing layer	$R_e \simeq 20000$
Ye *et al.* (1996)	Rayleigh-Bénard convection	$R_\lambda \simeq 8$-47 $P_r \simeq 0.006$-0.7

These databases contain complete three-dimensional random flow fields from which it is possible to extract any information required for checking physical ideas and fundamental assumptions that are used in the development of turbulence closure.

Dynamic equations of inhomogeneous anisotropic turbulence

The stress equation reads:

$$\frac{\partial \overline{u_i u_j}}{\partial t} + \overline{U}_k \frac{\overline{u_i u_j}}{\partial x_k} \cong P_{ij} + a_{ij} P_{ss} + \mathcal{F}\left(\frac{1}{3} P_{ss}\delta_{ij} - P_{ij}\right) + (\mathcal{C} - 2\mathcal{A}\epsilon_h) a_{ij} - \frac{2}{3}\epsilon_h \delta_{ij}$$
$$+ c_q \frac{\partial}{\partial x_k} \frac{\overline{u_i u_j}}{q^2} \frac{k^2}{\epsilon_h} J \frac{\partial k}{\partial x_k} + \frac{1}{2}\nu \frac{\partial^2 \overline{u_i u_j}}{\partial x_k \partial x_k}$$

The dissipation equation can be approximated as:

$$\frac{\partial \epsilon_h}{\partial t} + \overline{U}_k \frac{\partial \epsilon_h}{\partial x_k} \cong -2\mathcal{A} \frac{\epsilon_h \overline{u_i u_k}}{k} \frac{\partial \overline{U_i}}{\partial x_k} - \psi \frac{\epsilon_h^2}{k} + c_\epsilon \frac{\partial}{\partial x_k} \frac{k^2}{\epsilon_h} J \frac{\partial \epsilon_h}{\partial x_k} + \frac{1}{2}\nu \frac{\partial^2 \epsilon_h}{\partial x_k \partial x_k}$$

$$\mathcal{A} \simeq 1 + \underbrace{\left\{1 - 9\left[\frac{1}{2}\mathrm{II}_a - \mathrm{III}_a\right]\right\}}_{J} (\mathcal{W} - 1)$$

$$\mathcal{F} \simeq \frac{3}{5} + \frac{18}{5}\left(\frac{1}{2}\mathrm{II}_a - \mathrm{III}_a\right)$$

$$\mathcal{C} \simeq [1 - 9(\tfrac{1}{2}\mathrm{II}_a - \mathrm{III}_a)](4.78\mathcal{W} - 4.78)\epsilon_h$$

$$\psi \approx (1 - F)(\psi)_{2C} + F(\psi)_{\mathrm{axi}}$$

$$F = \frac{1 - 9(\frac{1}{2}\mathrm{II}_a - \mathrm{III}_a)}{1 - 9[\frac{3}{4}(\frac{4}{3}|\mathrm{III}_a|)^{2/3} - \mathrm{III}_a]}$$

$$(\psi)_{2C} \approx \frac{\sqrt{5}}{25} R_\lambda \mathcal{W} + 2(1 - \mathcal{W})$$

$$(\psi)_{\mathrm{axi}} \approx \left\{1 - 9\left[\frac{3}{4}\left(\frac{4}{3}|\mathrm{III}_a|\right)^{2/3} - \mathrm{III}_a\right]\right\}(1.8 - 0.4\mathrm{W}), \quad \mathrm{III}_a \geq 0$$

$$(\psi)_{\mathrm{axi}} \approx 2.5 - \left\{1 - 9\left[\frac{3}{4}\left(\frac{4}{3}|\mathrm{III}_a|\right)^{2/3} - \mathrm{III}_a\right]\right\}(0.7 + 0.5\mathcal{W}), \quad \mathrm{III}_a \leq 0$$

$$\frac{\lambda}{L} \simeq -0.0489 R_\lambda + \frac{1}{2}(0.00956 R_\lambda^2 + 10.186)^{1/2}$$

$$\mathcal{W} = 0.626 \frac{\lambda}{L}$$

$$c_\epsilon \approx \mathbf{0.09}$$

The statistical dynamics of turbulent stresses in a channel flow

The stress equations for a fully developed channel flow:

$$\frac{\partial \overline{u_1^2}}{\partial t} \simeq P_{11} + a_{11}P_{ss} + \mathcal{F}(\frac{1}{3}P_{ss} - P_{11}) + (\mathcal{C} - 2\mathcal{A}\epsilon_h)a_{11} - \frac{2}{3}\epsilon_h - \frac{\partial}{\partial x_2}\frac{\overline{u_1^2}}{q^2}\overline{u_s u_s u_2} + \frac{1}{2}\nu \frac{\partial^2 \overline{u_1^2}}{\partial x_2^2}$$

$$\frac{\partial \overline{u_2^2}}{\partial t} \simeq a_{22}P_{ss} + \frac{1}{3}\mathcal{F}P_{ss} + (\mathcal{C} - 2\mathcal{A}\epsilon_h)a_{22} - \frac{2}{3}\epsilon_h - \frac{\partial}{\partial x_2}\frac{\overline{u_2^2}}{q^2}\overline{u_s u_s u_2} + \frac{1}{2}\nu \frac{\partial^2 \overline{u_2^2}}{\partial x_2^2}$$

$$\frac{\partial \overline{u_3^2}}{\partial t} \simeq a_{33}P_{ss} + \frac{1}{3}\mathcal{F}P_{ss} + (\mathcal{C} - 2\mathcal{A}\epsilon_h)a_{33} - \frac{2}{3}\epsilon_h - \frac{\partial}{\partial x_2}\frac{\overline{u_3^2}}{q^2}\overline{u_s u_s u_2} + \frac{1}{2}\nu \frac{\partial^2 \overline{u_3^2}}{\partial x_2^2}$$

$$\frac{\partial \overline{u_1 u_2}}{\partial t} \simeq P_{12} + a_{12}P_{ss} - \mathcal{F}P_{12} + (\mathcal{C} - 2\mathcal{A}\epsilon_h)a_{12} - \frac{\partial}{\partial x_2}\frac{\overline{u_1 u_2}}{q^2}\overline{u_s u_s u_2} + \frac{1}{2}\nu \frac{\partial^2 \overline{u_1 u_2}}{\partial x_2^2}$$

Away from the wall the system resembles the statistical dynamics of initially isotropic turbulence strained by axisymmetric expansion.

Anisotropy invariant mapping of turbulence in a channel flow

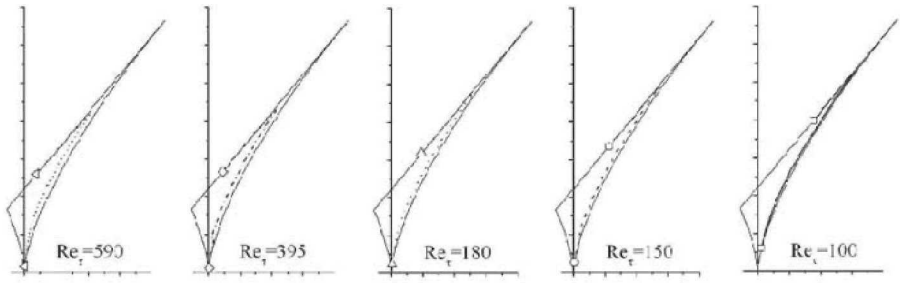

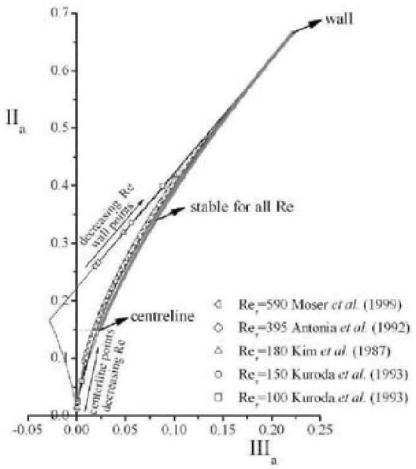

- The shading indicates the area occupied by the stable disturbances: for such disturbances it is expected that the laminar regime in the flat plate boundary layer will persist up to very high Reynolds numbers.

The limiting state of turbulence at the wall

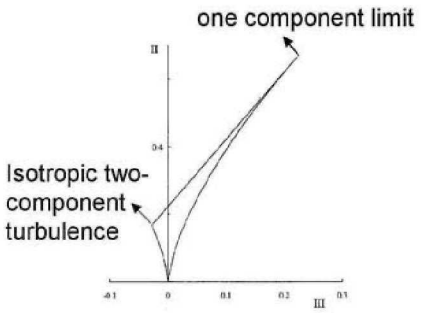

Expansion of velocity fluctuations near the wall:

$$u_1 = a_1 x_2 + a_2 x_2^2 + a_3 x_2^3 + \ldots..$$
$$u_2 = \quad b_2 x_2^2 + b_3 x_2^3 + \ldots..$$
$$u_3 = c_1 x_2 + c_2 x_2^2 + c_3 x_2^3 + \ldots..$$

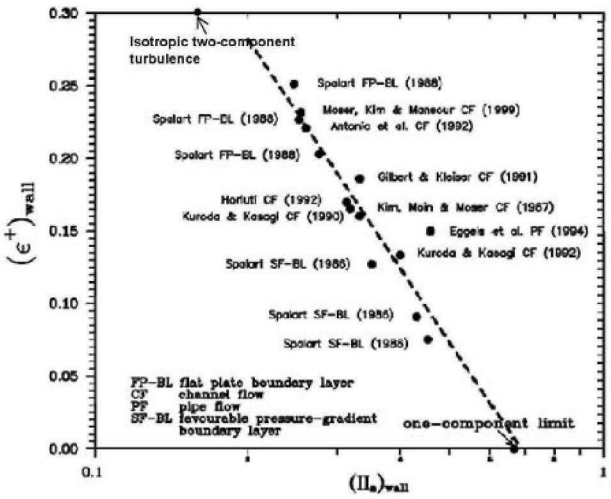

Numerical data bases confirm that ε vanishes as the one-component state is approached

- Requesting that $\overline{u_i u_j}$ and ε_{ij} are statistically axisymmetric we find that

$$a_1, b_2, c_1, \ldots a_n, b_{n+1}, c_n \to 0 \quad \text{and} \quad k = \frac{1}{2}\frac{(\varepsilon)_{\text{wall}}}{\nu} x_2 \,, (\varepsilon)_{\text{wall}} = \nu\left(\overline{a_1^2} + \overline{c_1^2}\right) \to 0 \quad \text{as} \quad x_2 \to 0$$

Anisotropy-invariant mapping of turbulence with drag reduction

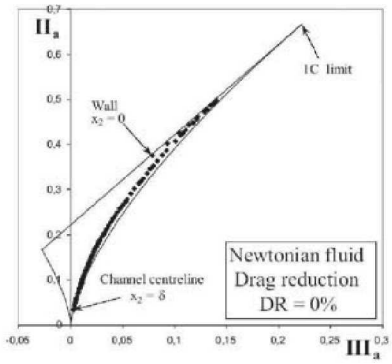

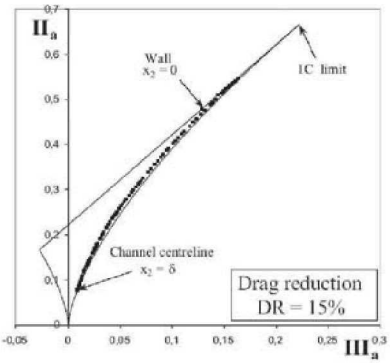

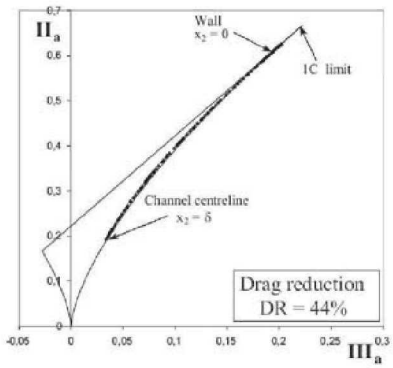

The trend in the data at the wall strongly support the conclusion that DR increases as turbulence approaches the one component limit.

Polymer-turbulence interaction (I)

The polymer molecule in solution at equilibrium

monomer of length l N monomers of length l

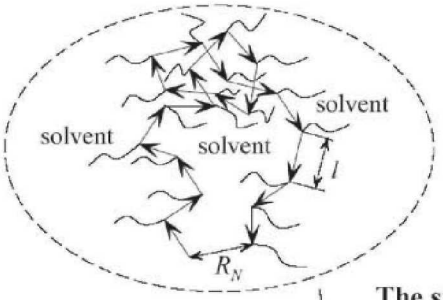

$$R_F = N^{3/5} l$$

$$(t_{Zimm})_{pol} = \frac{\eta_s R_F^3}{k_B T}$$

η_s - the solvent viscosity
k_B - Bolzmann constant
T - absolute temperature

The stretched polymer molecule in the near-wall region of turbulent pipe flow

$$(t)_{pol} \geq (t)_{tur}$$

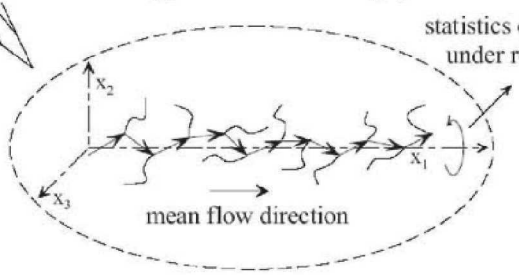

Polymer turbulence interaction (II)

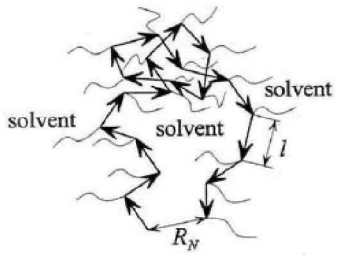

$t_{tur} \leq t_{pol}$

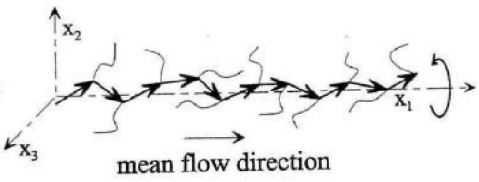

restructuring of small scale turbulence

conceptual scenario

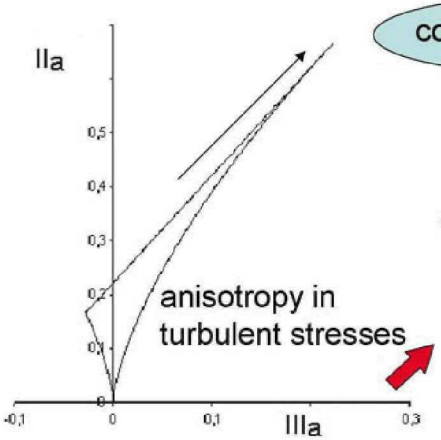

anisotropy in turbulent stresses

at the wall

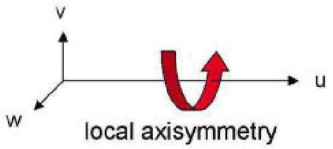

local axisymmetry

anisotropy in length scales

Maximum drag reduction

Theoretical Prediction

max DR for $t_{tur} \approx t_K \leq t_{pol}$ $\qquad (t_K)_{Wall} = \frac{\eta_K^2}{\upsilon} \approx \sqrt{10}\,\frac{\upsilon}{u_\tau^2}$

Deborah number $De(DR_{\max}) \geq \sqrt{10}$

Experimental Results (Durst et al. 1982)

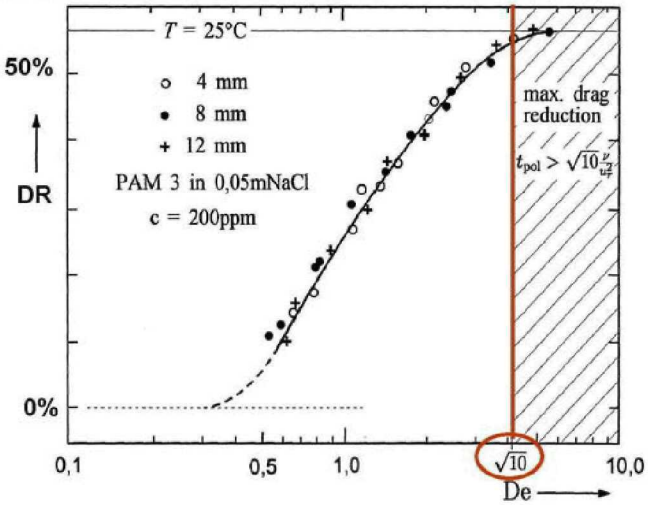

Direct simulations of near-wall turbulence

Kim, Moin and Moser, Nasa Ames Research Center, 1986

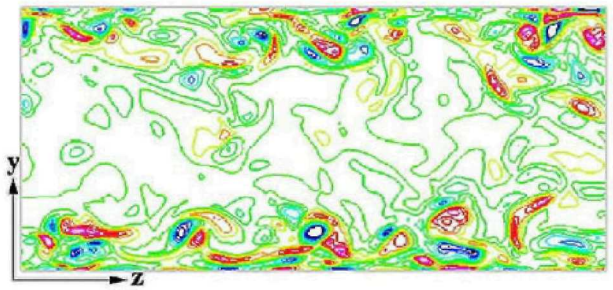

Color contours of the streamwise vorticity in the direct numerical simulations of fully developed channel flow

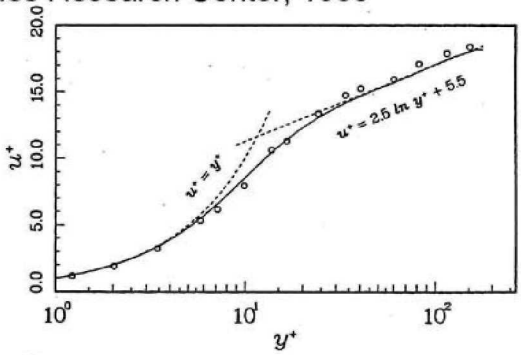

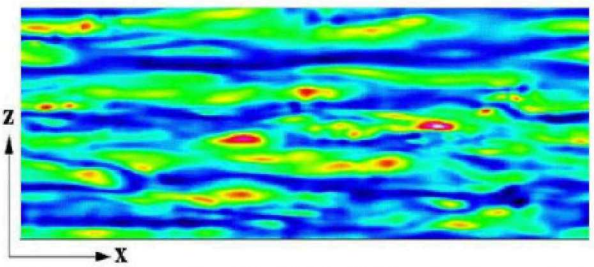

Color shades of the skin friction in the direct numerical simulations of fully developed channel flow

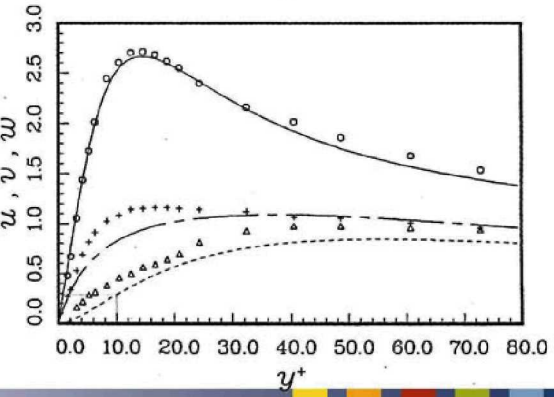

Direct simulations of near-wall turbulence

Kim, Moin and Moser, Nasa Ames Research Center, 1986

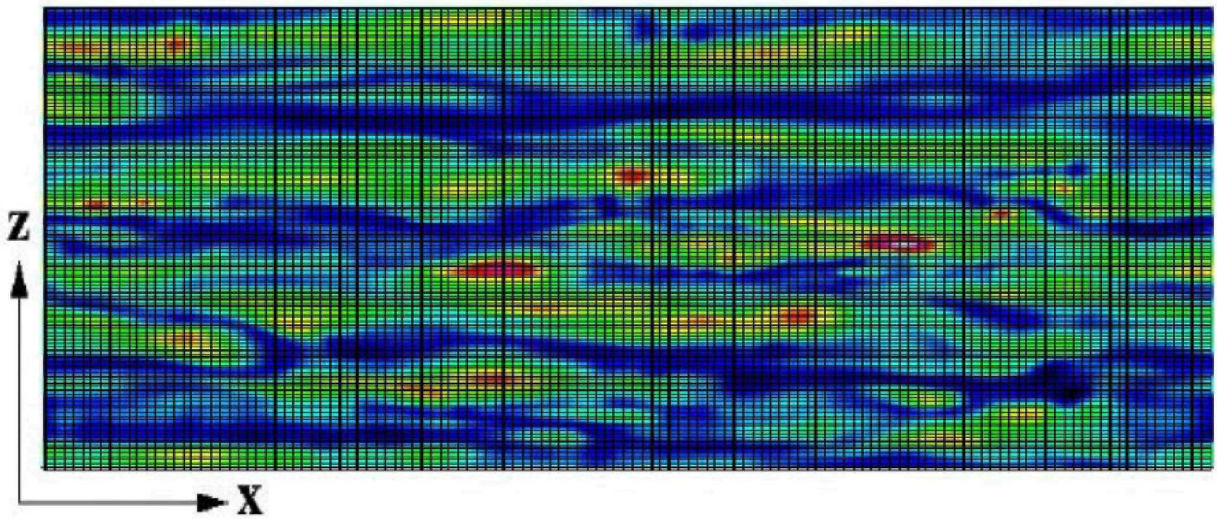

The optimum concentration

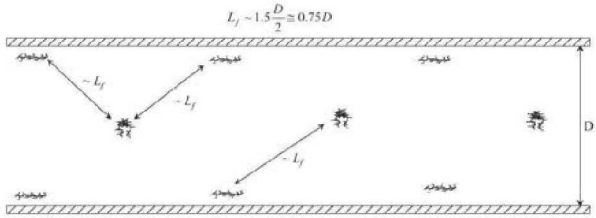

Interaction between polymer and turbulence in dissipation range (η_k):

$$\frac{c_{POL}}{V} \approx \left(\frac{\eta_K}{L_f}\right)^3$$

$Re \uparrow \Rightarrow \frac{c}{V} \downarrow$

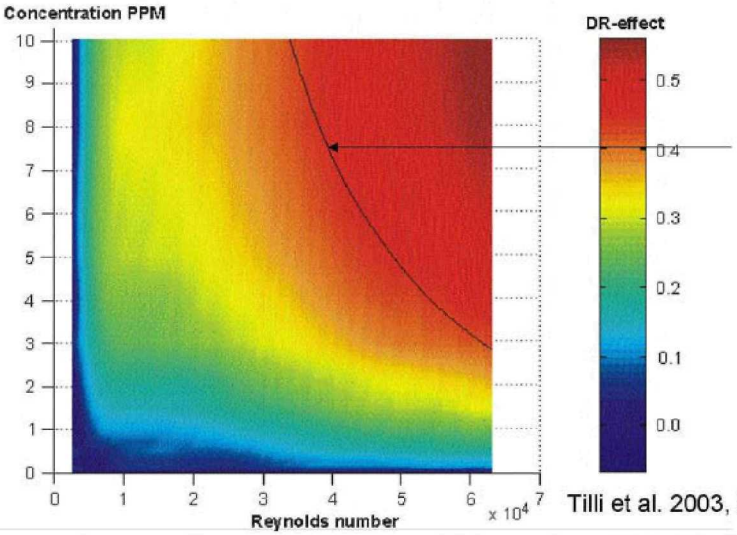

prediction of polymer concentration for max DR

Tilli et al. 2003, PAA

Experimental Investigation

refractive index matched pipe flow facility

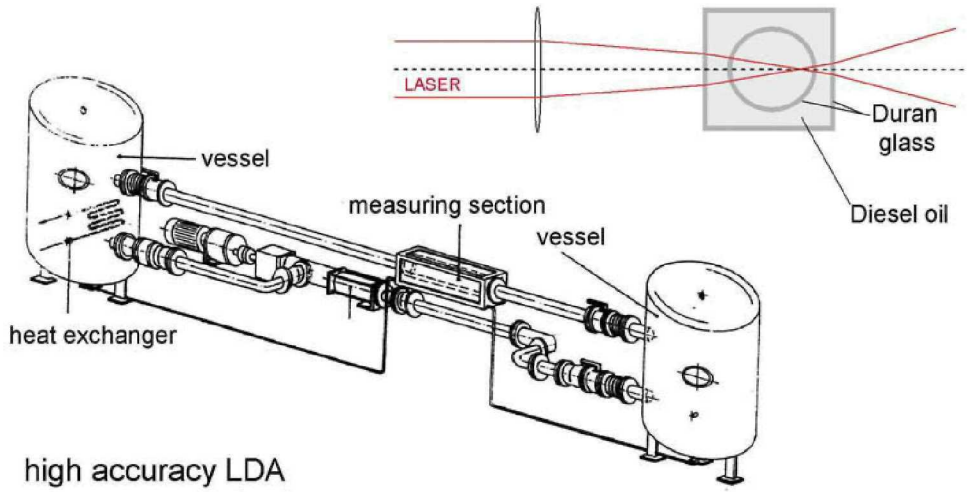

high accuracy LDA measurements in the viscous sublayer, y=150µm

Measured quantities

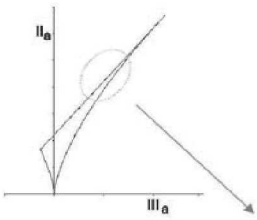

Anisotropy tensor

$$a_{ij} = \frac{\overline{u_i u_j}}{q^2} - \frac{1}{3}\delta_{ij}$$

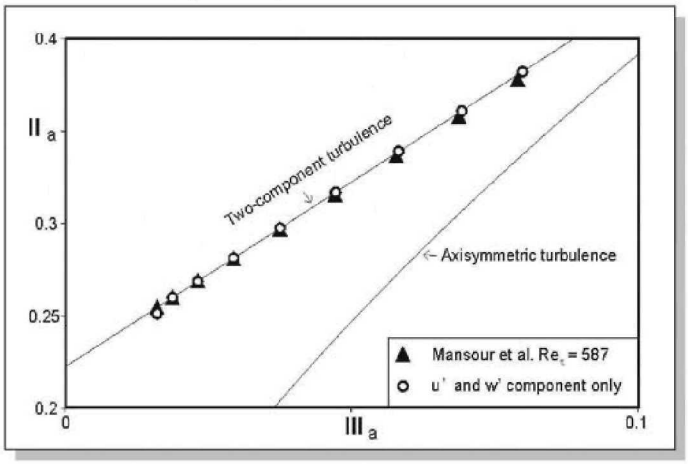

for points in viscous sublayer a_{ij} can be based on **u' and w' component** only

Drag Reduction DR

$$DR = 1 - \frac{\tau_{w,pol}}{\tau_w}$$

$$\tau_w = \mu \frac{\partial U}{\partial x}$$

in viscous sublayer it holds:

$$y^+ = U^+$$

$$y = C \cdot U$$

measure **mean velocity U** in one point of viscous sublayer

The molecular structure of a polymer sample

Illustration of the molecular structure of a FORTUM polymer sample

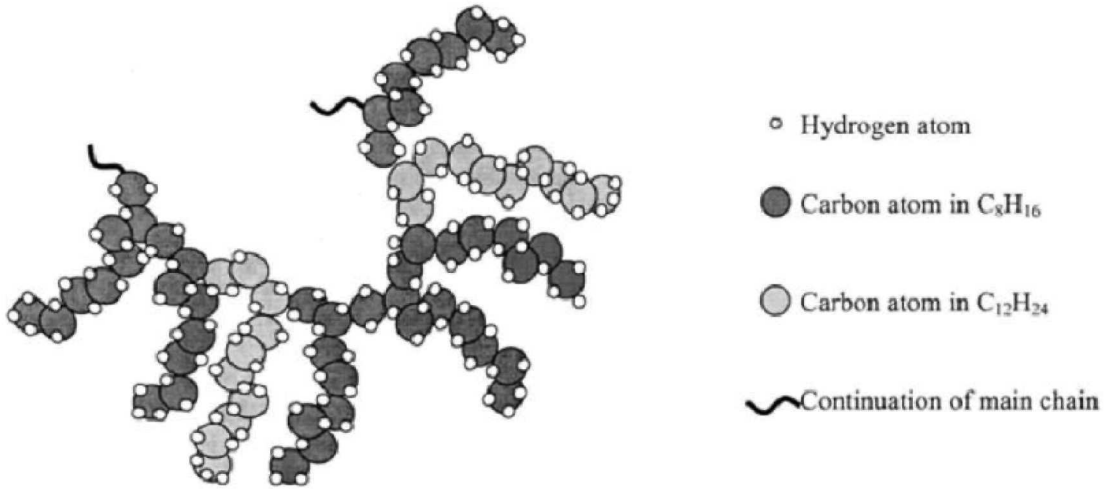

$M \approx 25\times10^6$ g mol^{-1}, $M_{dodecane} = 168.4320$ g mol^{-1}, $M_{octane} = 112.2880$ g mol^{-1}, $l = 2 \times 1.54$ Å, $r_{d/o} - C_{12}H_{24}/C_8H_{16} - 1/3$, $N_{monomer} - M_{polymer}/[r_{d/o}M_{octane} + (1 - r_{d/o})M_{dodecane}]$.

Experimental results

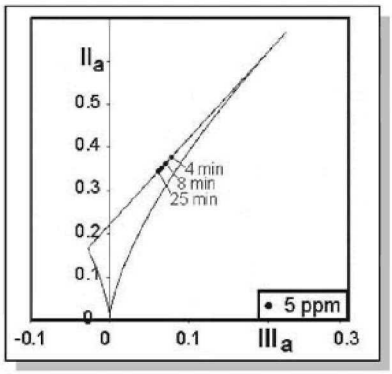

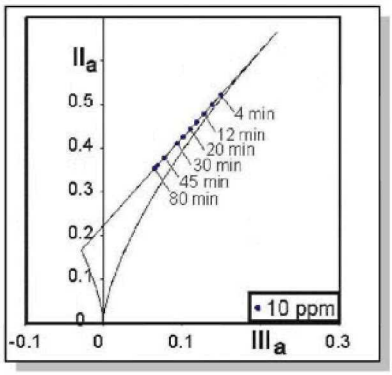

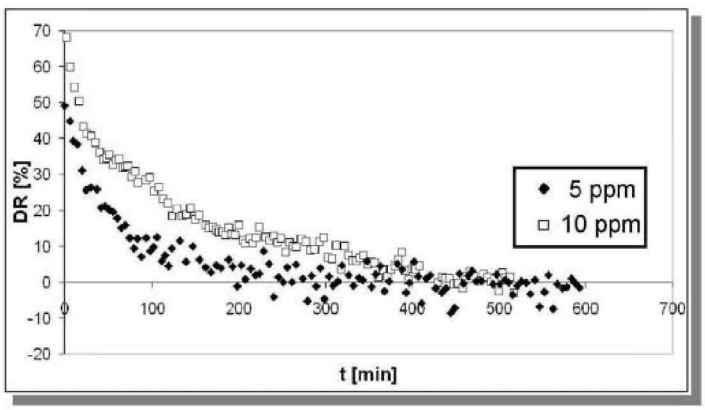

➡ Anisotropy decreases with the degradation of the polymer

The chief mechanism responsible for polymer drag reduction

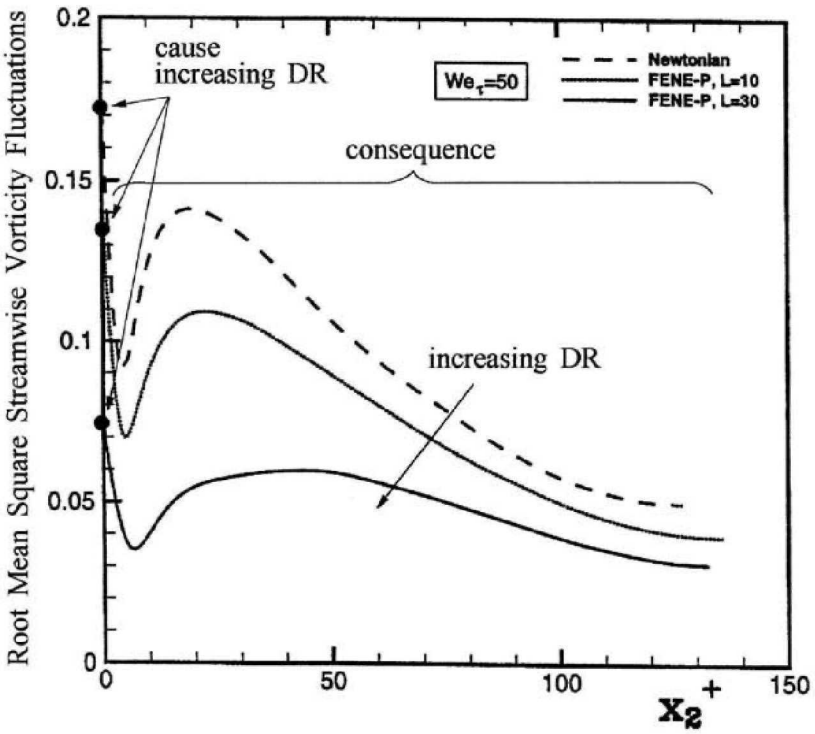

The mechanism responsible for turbulent drag reduction by high polymers

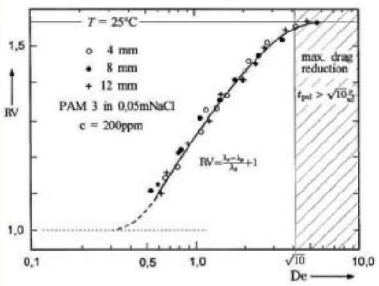

Drag reduction versus a polymer time scale

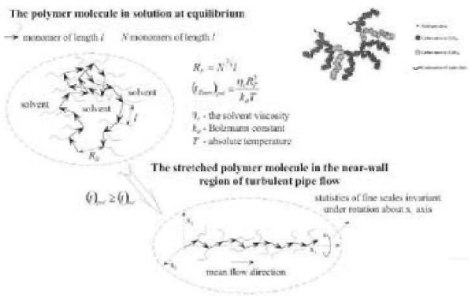

Behaviour of a polymer in a solution at equilibrium and its response to stretching by turbulent motions at small scales very close to the wall

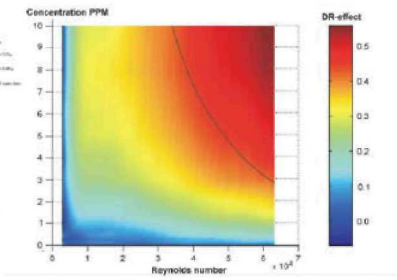

The optimum concentration of a polymer

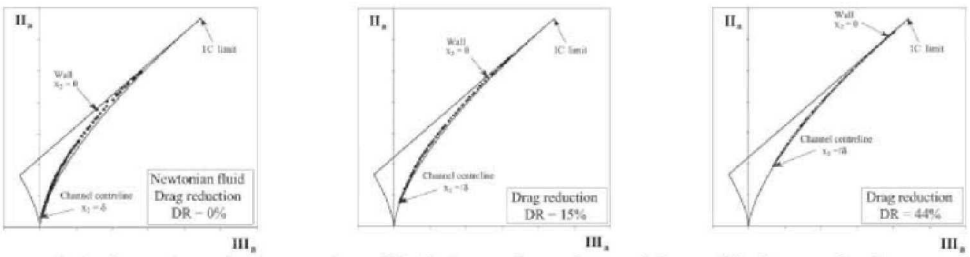

Anisotropy invariant mapping of turbulence in a channel flow with drag reduction

Turbulent drag reduction by riblets

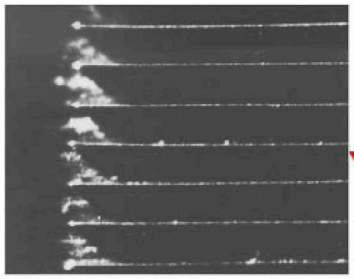

Top view of riblets

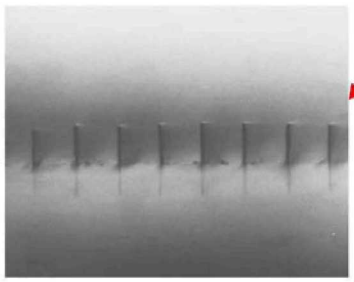

Front view of riblets

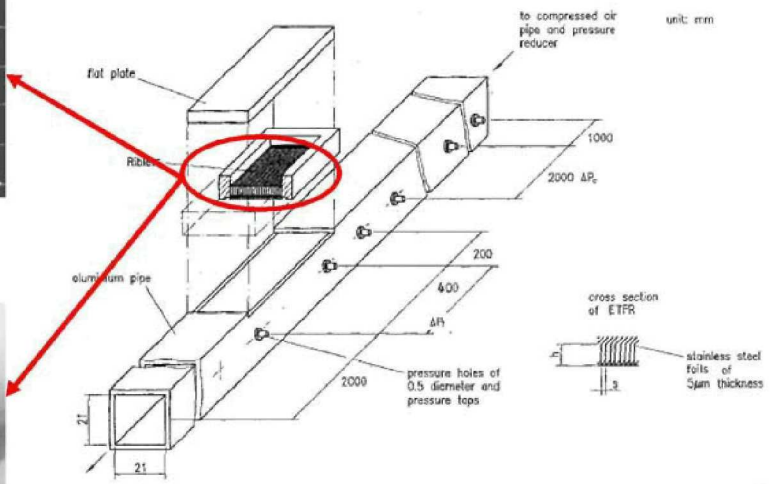

Schematic drawing of test section facility

Flow laminarization

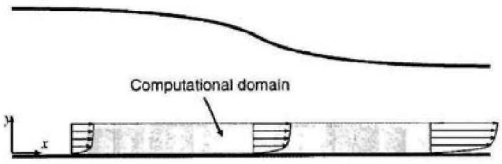

Sketch of the physical configuration

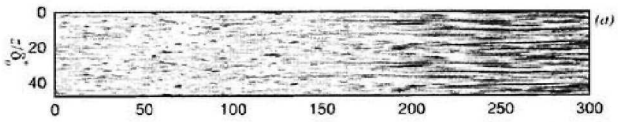

Instantaneous streamwise velocity fluctuations

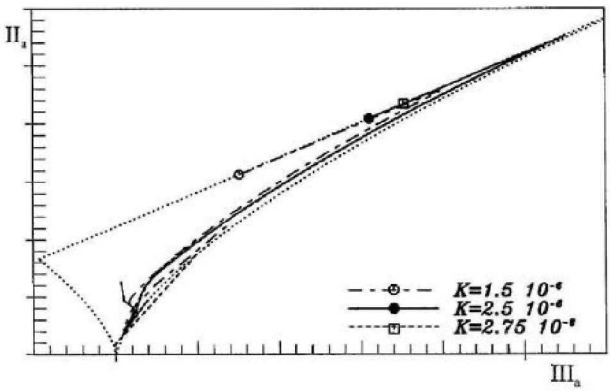

$$K = \frac{\nu}{U_\infty^2}\frac{dU_\infty}{dx}$$

$$(K)_{crit} \geq 3.75 \times 10^{-6}$$

Traces of the joint variations of the invariants for a turbulent boundary layer developing under favorable pressure gradient

Compressibility effect in supersonic wall-bounded flows

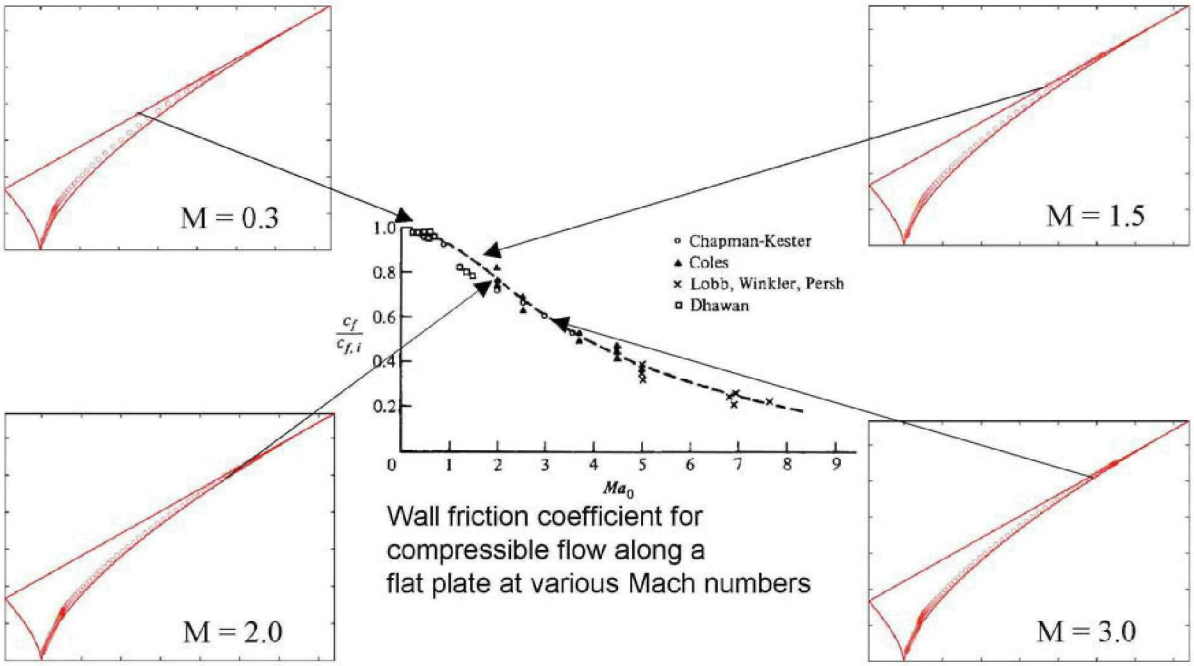

Wall friction coefficient for compressible flow along a flat plate at various Mach numbers

The origin of turbulence in wall-bounded flows (I)

Cantwell, Coles, Dimotakis JFM 87, 1978

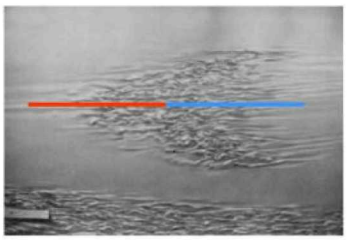

low Reynolds number

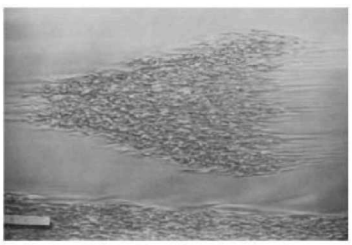

high Reynolds number

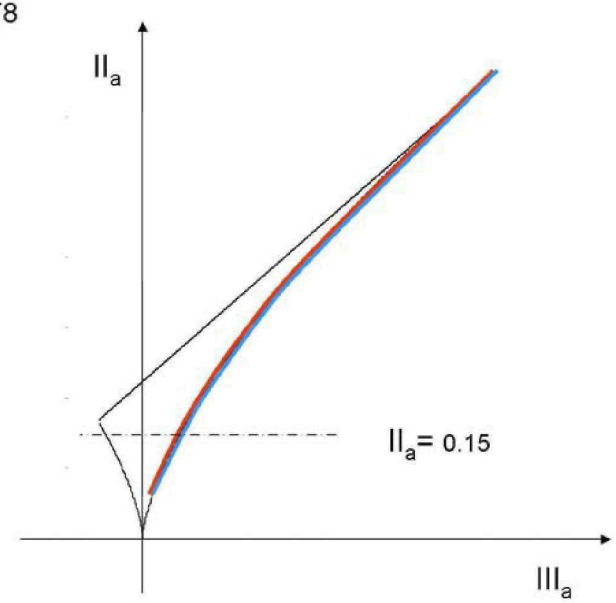

Note that transition and breakdown to turbulence is associated with decrease of anisotropy at the front side of the spot and laminarization process proceeds with Increase of the anisotropy at the trailing side of the spot.

The origin of turbulence in wall-bounded flows (II)

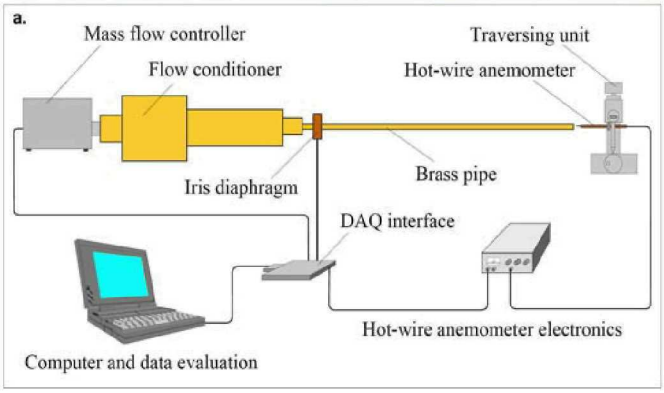

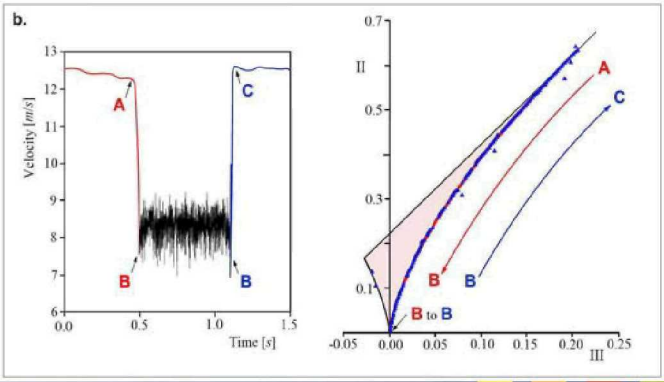

The origin of turbulence in wall-bounded flows (III)

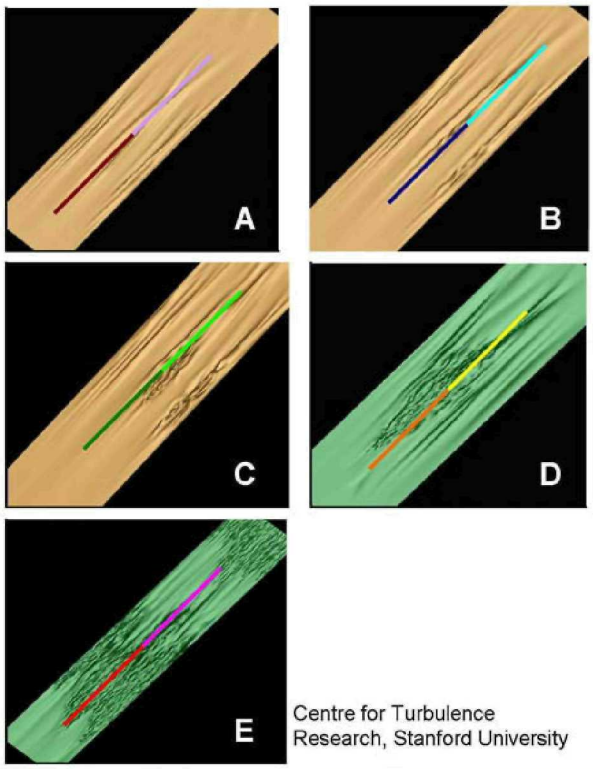

Centre for Turbulence Research, Stanford University

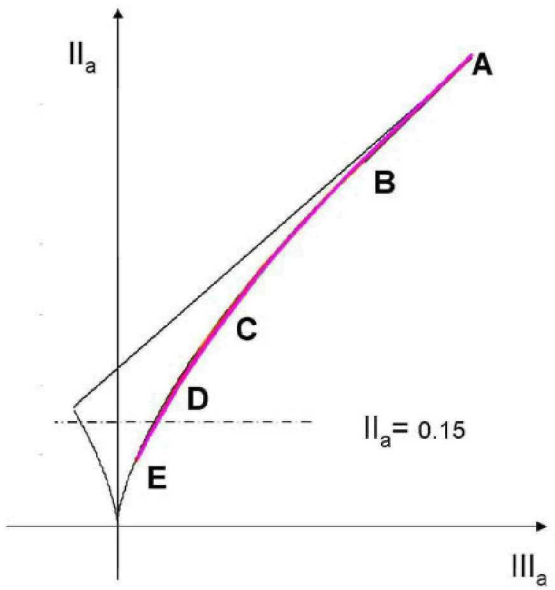

Virtual Channel Flow (I)

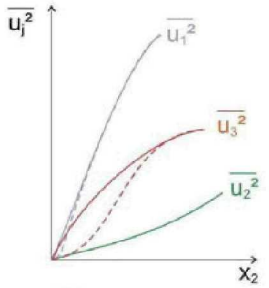

Channel Flow (Re_τ=180) with artificial boundary conditions:
Points in the viscous sub layer were modified: u3→u2

⟶ τ_w takes on the following

⟶ $$DR = 1 - \left(\frac{\tau_w}{(\tau_w)_{unforced}} \right)$$

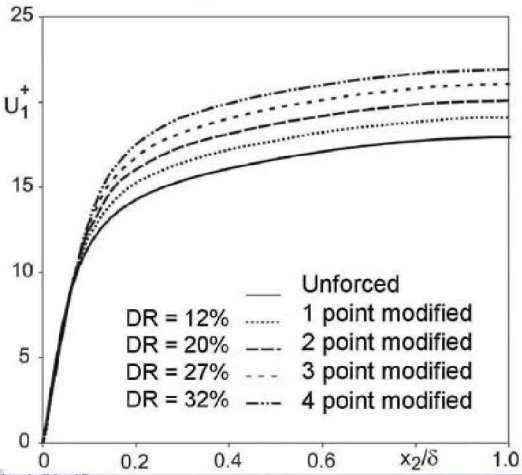

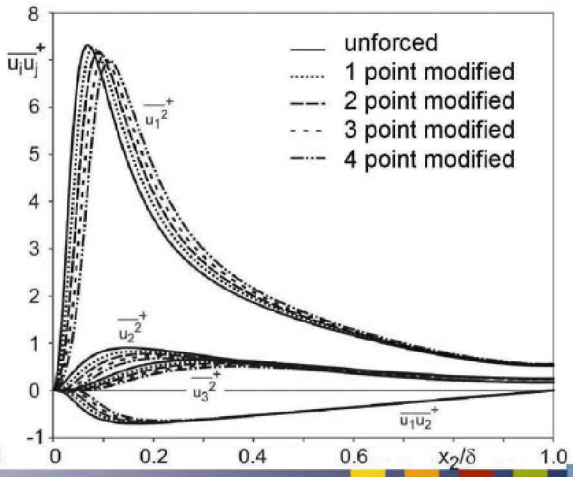

Virtual Channel Flow (II)

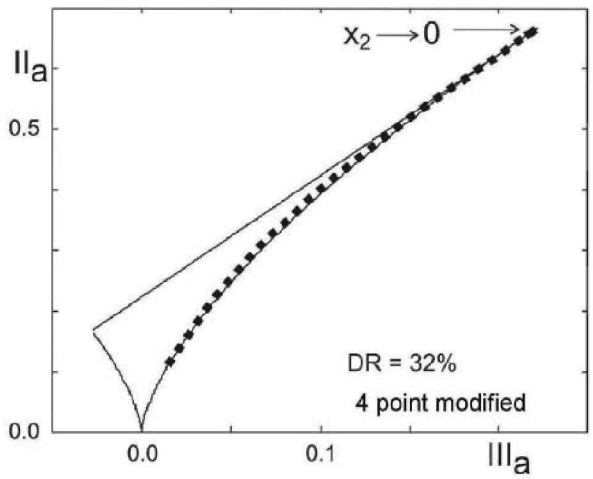

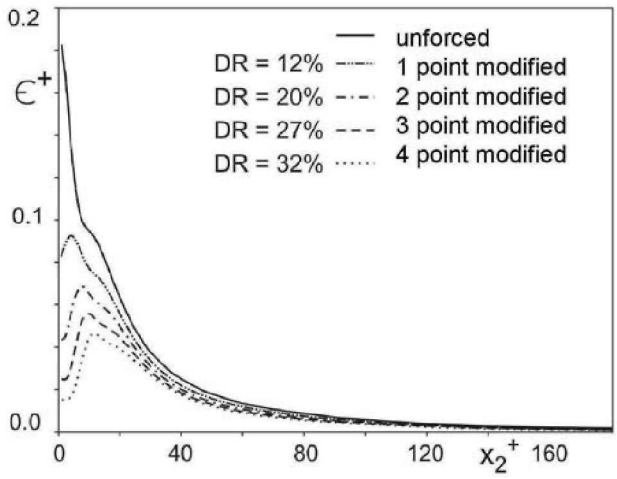

Small variations near the wall lead to significant drag reduction

Numerical experiments on wall turbulence

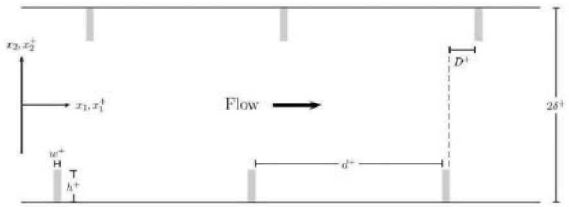

Configuration of the roughness elements mounted at the walls of a plane channel flow

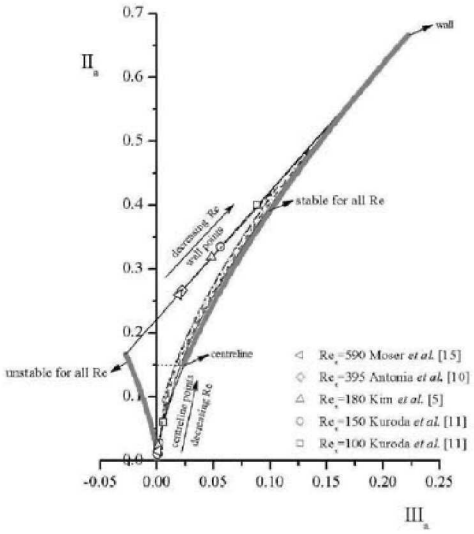

Anisotropy invariant mapping of turbulence in a plane channel flow at low Reynolds numbers

Simulation results

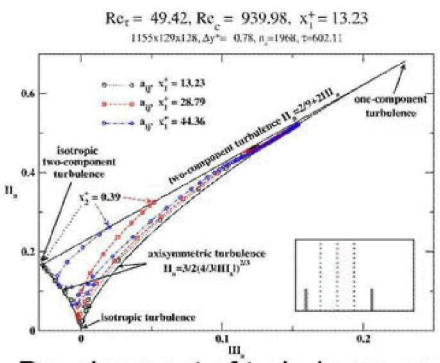

Development of turbulence across the anisotropy invariant map

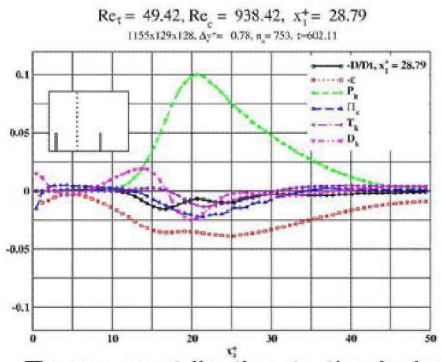

Terms contributing to the balance of the energy equation

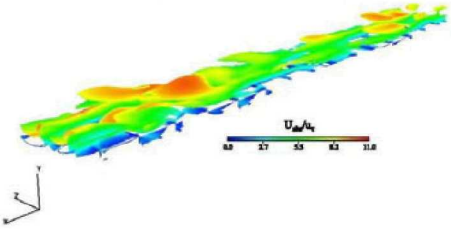

Isosurface of instantaneous vorticity at Re = 940

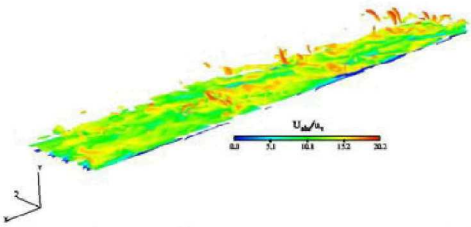

Isosurface of instantaneous vorticity at Re = 6600

Numerical simulation of complex turbulent flows

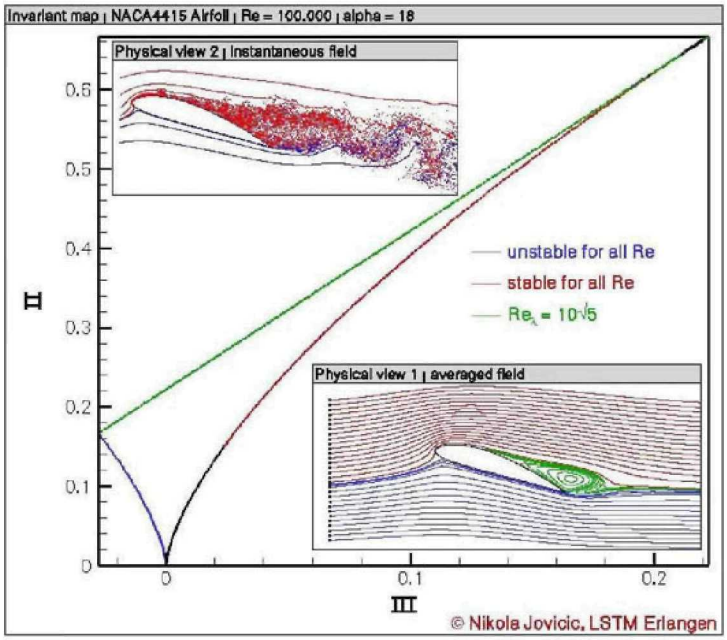

To start the video, click on the picture!

Drag reduction by surface-embedded grooves

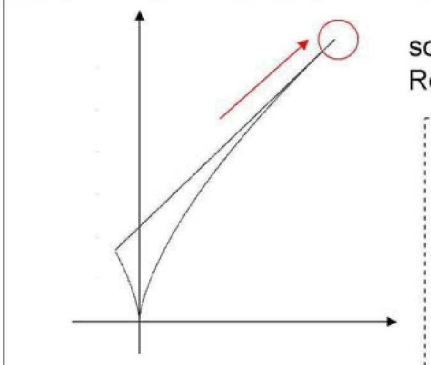

scientific goal and “engineering dream”:
Realize one-component limit at the wall and obtain very high DR

one possible technical realization:
channel flow with surface modification

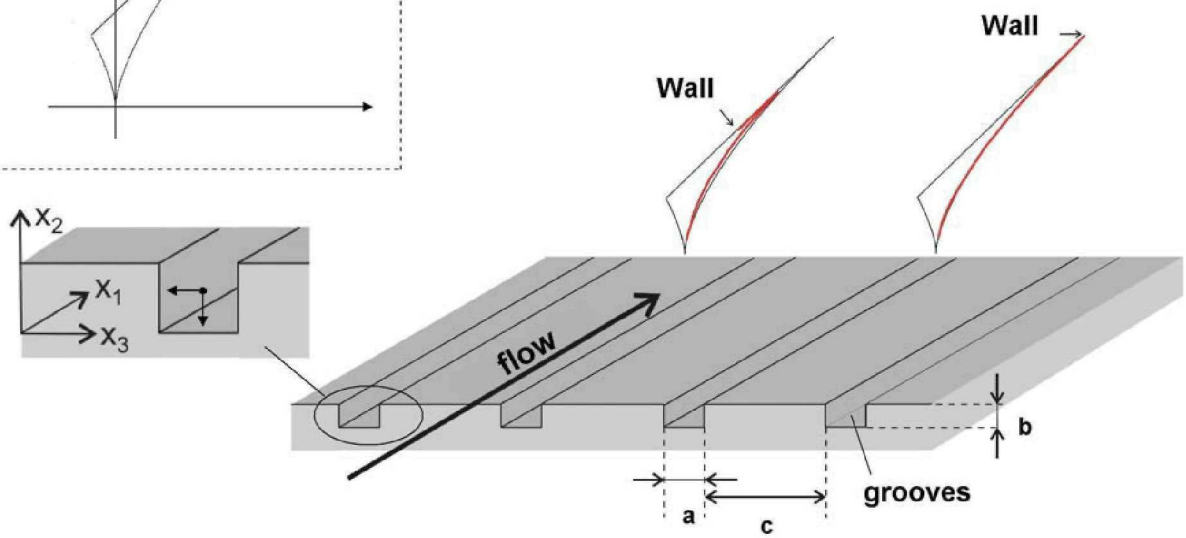

Flow in the Grooves (I)

Basic equations for fully developed flow in a groove

$$\frac{\partial \overline{U}_2}{\partial x_2} + \frac{\partial \overline{U}_3}{\partial x_3} = 0$$

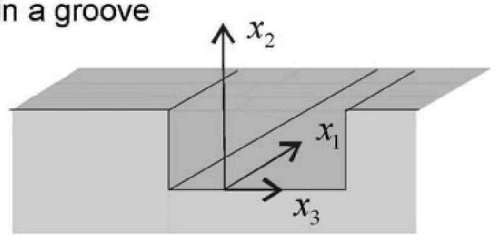

$$\overline{U}_2 \frac{\partial \overline{U}_1}{\partial x_2} + \overline{U}_3 \frac{\partial \overline{U}_1}{\partial x_3} = -\frac{1}{\rho}\frac{\partial \overline{P}}{\partial x_1} - \frac{\partial \overline{u_1 u_2}}{\partial x_2} - \frac{\partial \overline{u_1 u_3}}{\partial x_3} + \nu\left(\frac{\partial^2 \overline{U}_1}{\partial x_2^2} + \frac{\partial^2 \overline{U}_1}{\partial x_3^2}\right) \quad (1)$$

$$\overline{U}_2 \frac{\partial \overline{U}_2}{\partial x_2} + \overline{U}_3 \frac{\partial \overline{U}_2}{\partial x_3} = -\frac{1}{\rho}\frac{\partial \overline{P}}{\partial x_2} - \frac{\partial \overline{u_2^2}}{\partial x_2} - \frac{\partial \overline{u_2 u_3}}{\partial x_3} + \nu\left(\frac{\partial^2 \overline{U}_2}{\partial x_2^2} + \frac{\partial^2 \overline{U}_2}{\partial x_3^2}\right) \quad (2)$$

$$\overline{U}_2 \frac{\partial \overline{U}_3}{\partial x_2} + \overline{U}_3 \frac{\partial \overline{U}_3}{\partial x_3} = -\frac{1}{\rho}\frac{\partial \overline{P}}{\partial x_3} - \frac{\partial \overline{u_2 u_3}}{\partial x_2} - \frac{\partial \overline{u_3^2}}{\partial x_3} + \nu\left(\frac{\partial^2 \overline{U}_3}{\partial x_2^2} + \frac{\partial^2 \overline{U}_3}{\partial x_3^2}\right) \quad (3)$$

Rotta 1972

Flow in the Grooves (II)

no secondary motion: $\overline{U}_2 = \overline{U}_3 = 0$

from last slide, combine equations (2) and (3):

$$\frac{\partial^2\left(\overline{u_2^2} - \overline{u_3^2}\right)}{\partial x_2 \partial x_3} + \frac{\partial^2 \overline{u_2 u_3}}{\partial x_3^2} - \frac{\partial^2 \overline{u_2 u_3}}{\partial x_2^2} = 0$$

obvious solution that satisfies boundary conditions:
axisymmetric turbulence, where

$$\overline{u_2^2} = \overline{u_3^2} \quad \text{and} \quad \overline{u_2 u_3} = 0$$

with $\overline{u_1^2} > \overline{u_2^2} = \overline{u_3^2}$

For such a configuration of axisymmetric turbulence the wall is located at the 1C limit!

Numerical Simulation (I)

Simulation of a turbulent channel flow based on the Lattice Boltzmann Method

Flow Domain

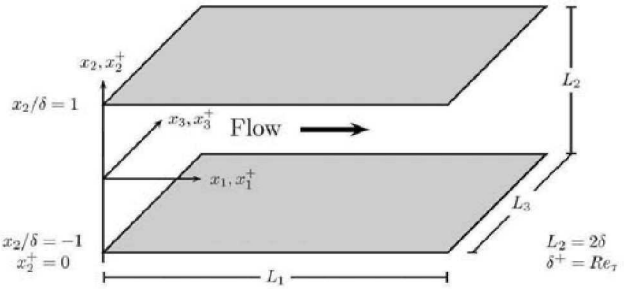

Model

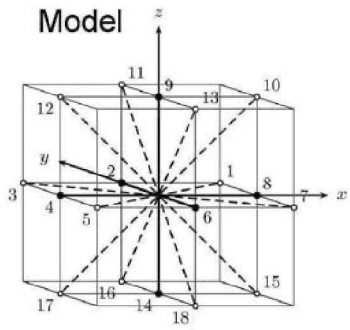

D3Q19

extremely high resolution with

$$N_1 \times N_2 \times N_3 = 4096 \times 364 \times 360$$

grid points possible

Dr. Peter Lammers, HLRS Stuttgart

Numerical Simulation (II)

Configurations for simulations with grooved walls:

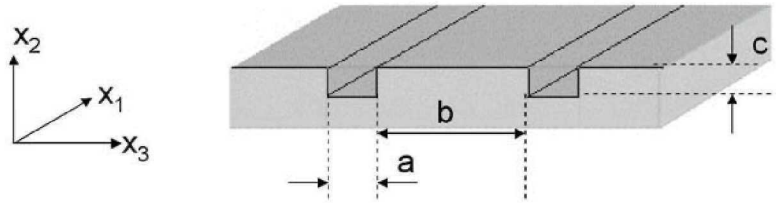

Reynolds number	resolution N1xN2xN3	resolution in wall units	a in wall units	b in wall units	c in wall units
6690	4096x264x240	1.4	8	13	5
6650	4096x264x240	1.4	5	14	5
5230	4096x364x360	0.8	4	15	4

Simulation Results

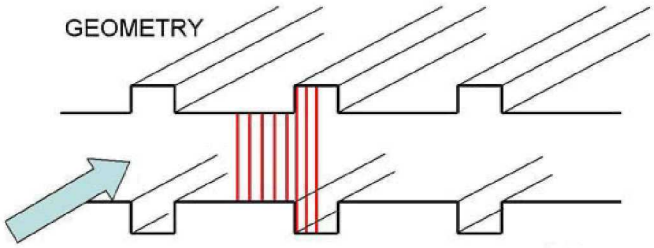

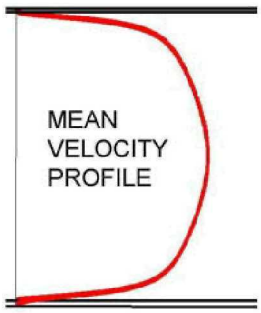

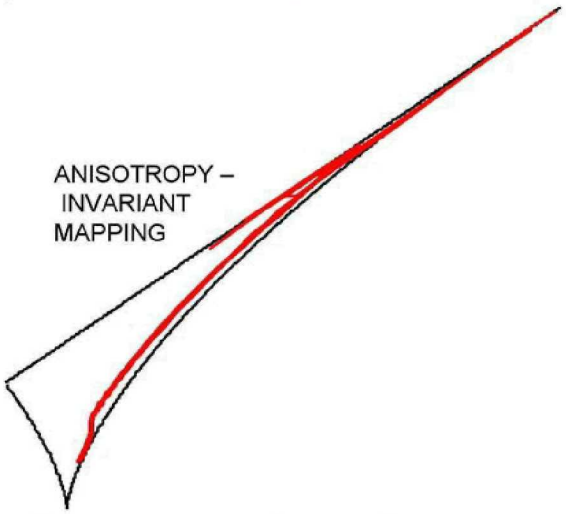

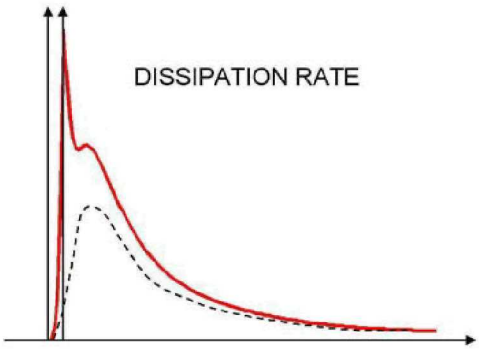

Simulated DR Effect

Reynolds number	a in wall units	b in wall units	c in wall units	DR simulation
6690	8	14	5	24%
6650	5	14	5	18%
5230	4	15	4	16%

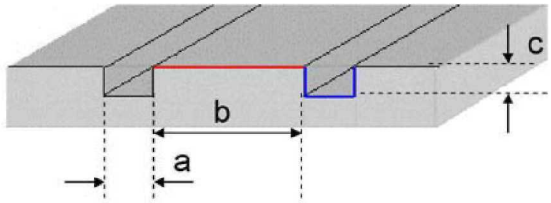

$$DR_{\max} \approx 1 - \frac{b}{a+b} = \frac{a}{a+b}$$

assumptions:

- DR as in flat channel
- negligible drag

Experimental Set-up

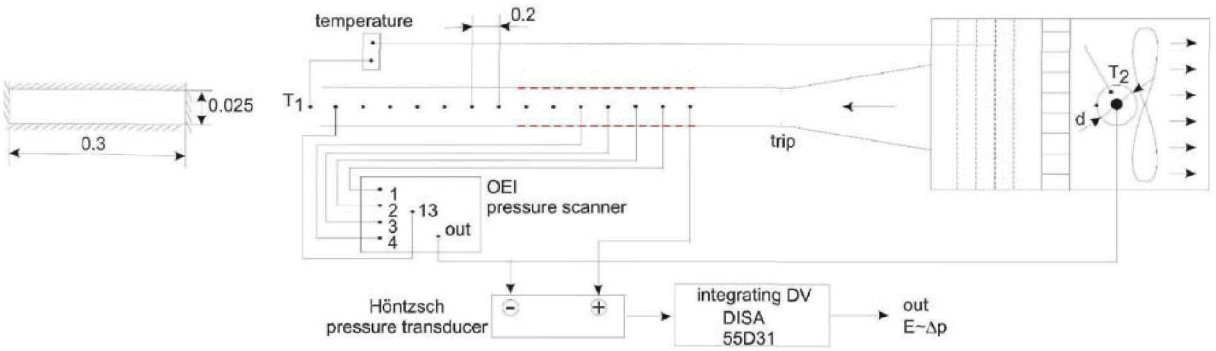

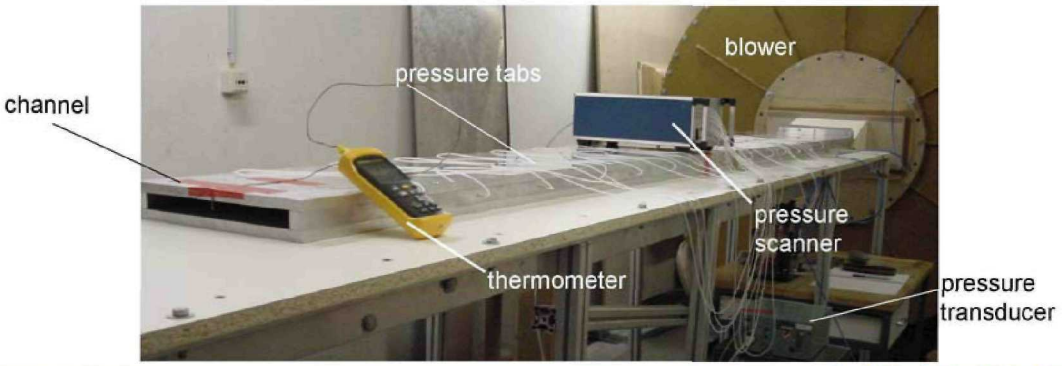

Test Plate with Grooves

non-polished surface

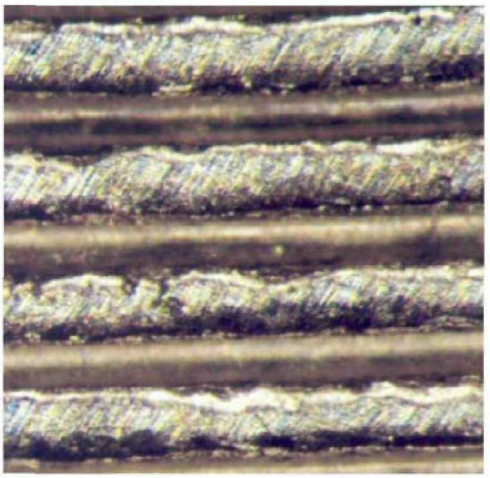

polished surface

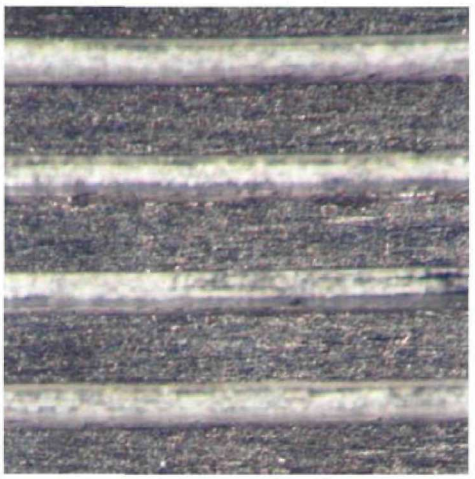

dimensions:

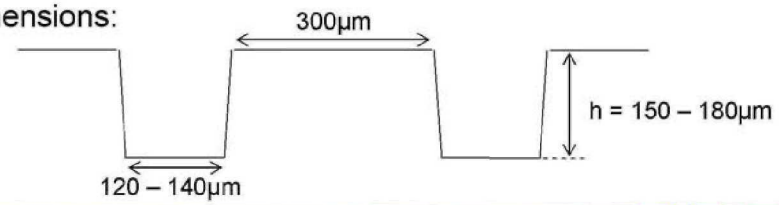

Measurements on Flat Plate

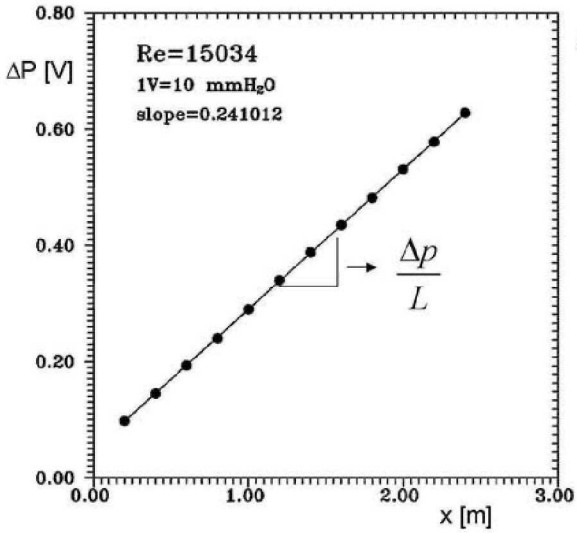

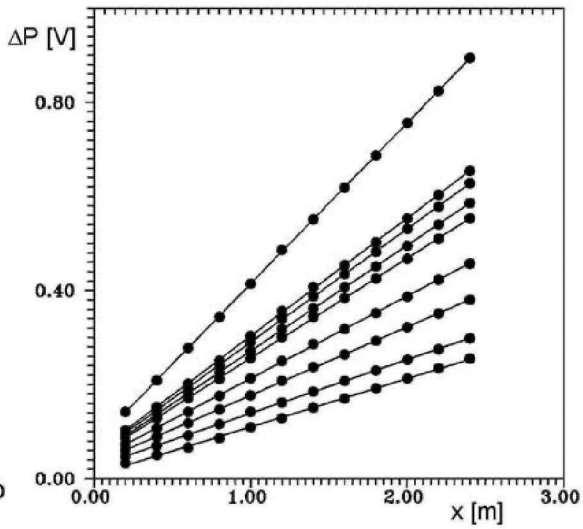

Measurements on Grooved Plate

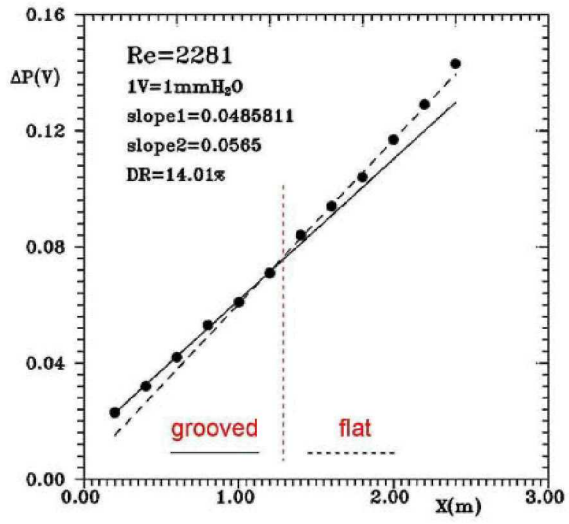

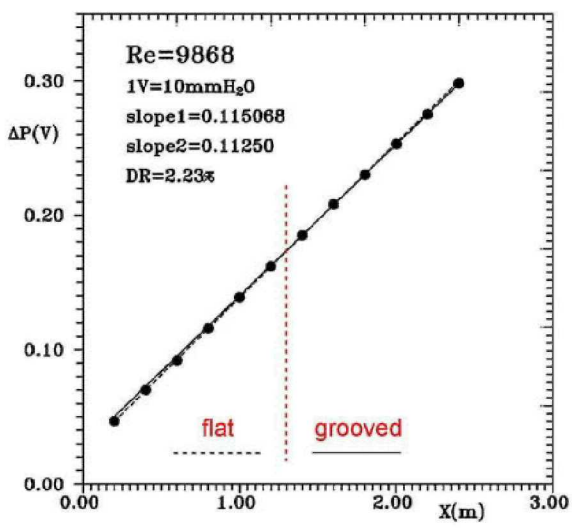

$$DR = 1 - \frac{slope_{grooved}}{slope_{flat}} = 1 - \frac{(\Delta p/\Delta L)_{grooved}}{(\Delta p/\Delta L)_{flat}}$$

Experimental Results

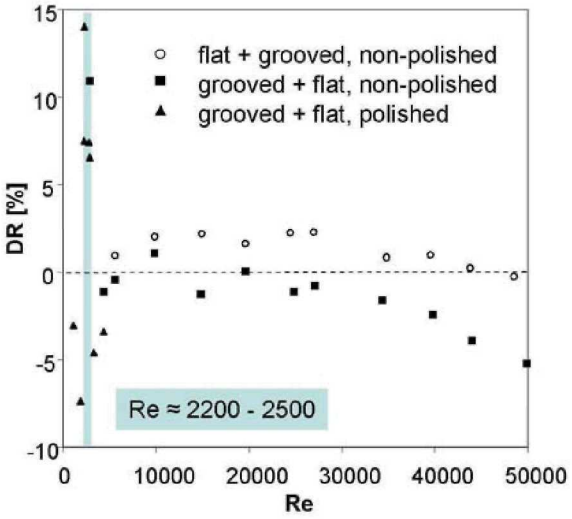

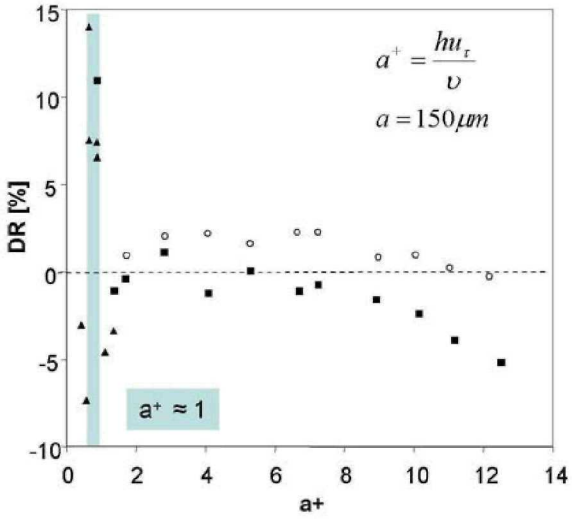

High DR values only in very narrow range around Re ≈ 2200 – 2550 and $a^+ \approx 1$

Kolmogorov scale $\eta_k^+ \approx 1.6$

New Experimental Result

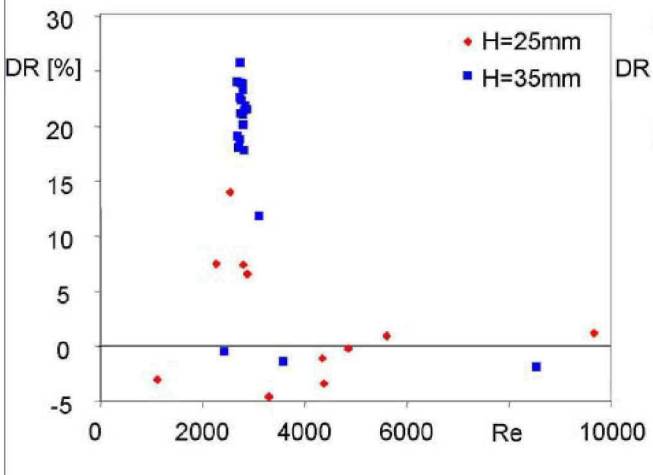

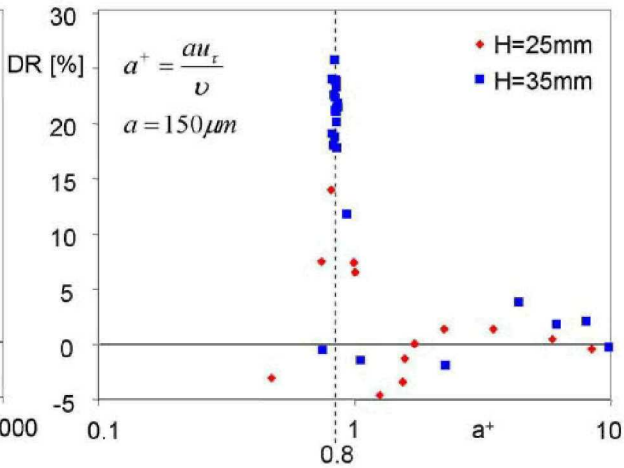

High DR is gained, when $a^+ \approx 0.8$

Kolmogorov Scale $\eta_k^+ \approx 1.5$

Conclusion

- Experiments and DNS data show increase in anisotropy with increasing DR
- DR is highest when 1C state is approached, where $(\varepsilon)_{wall}$ vanishes
- Trend explained with the scenario that polymers restructure dissipation range of spectrum (local axisymmetry)
- Experimental verification of the interaction level through prediction of optimum polymer concentration and its relaxation time for max DR
- Engineering use: determine best polymer and optimum concentration without trial and error
- Numerical simulations and experiments show that surface structuring can produce large DR effect which is very attractive for engineering implementation

Welcome at am Lehrstuhl für Strömungsmechanik

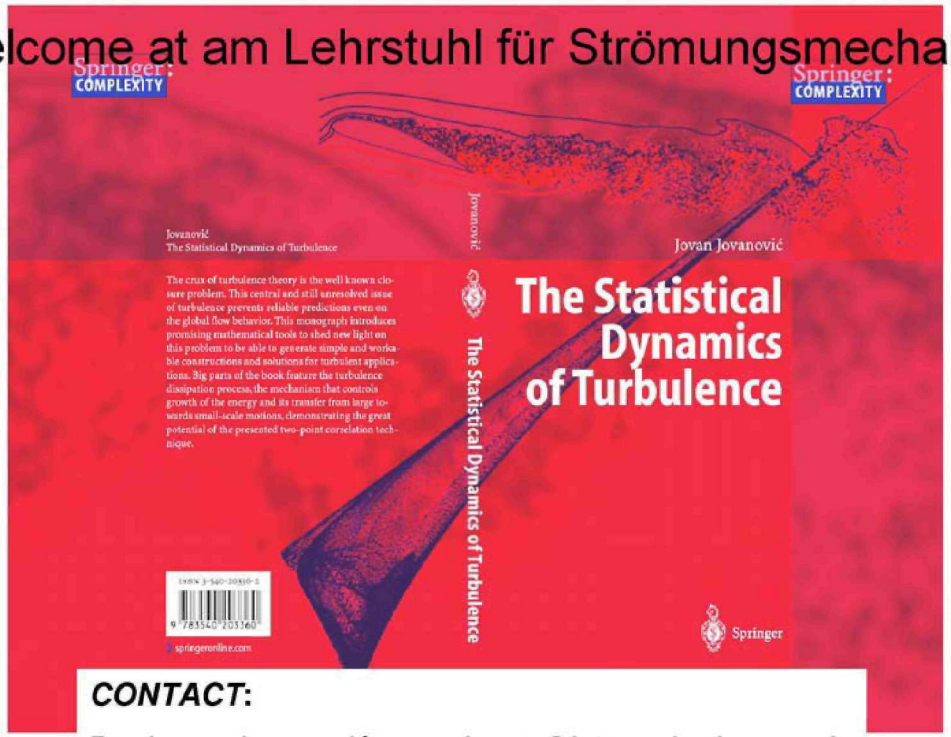

***CONTACT*:**

Dr. Jovan Jovanović jovan@lstm.uni-erlangen.de

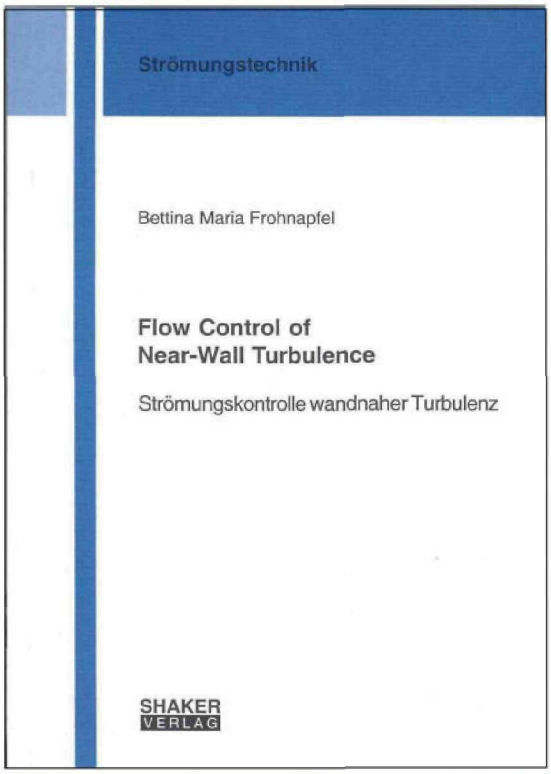

CONTACT:

Bettina Maria Frohnapfel
bettina@gmx.de